# A PDF METHOD FOR TURBULENT RECIRCULATING FLOWS

M. S. Anand*, S. B. Pope**, and H. C. Mongia*

* Allison Gas Turbine Division
General Motors Corporation
P.O. Box 420
Indianapolis, Indiana 46206

**Sibley School of Mechanical and Aerospace Engineering
Upson Hall, Cornell University
Ithaca, New York 14853

## ABSTRACT

A novel approach for the application of probability density function (PDF) methods to multidimensional turbulent recirculating flows is presented. The method is applicable to turbulent recirculating and reacting flows such as in gas turbine combustors. The method is based on a judicious combination of the conventional finite-volume technique for the solution of the Reynolds-averaged equations and the Monte Carlo technique for the solution of the transport equation for the velocity-scalar joint PDF. An important aspect of the approach is that the use of conventional turbulence closure models is avoided. The method is applied to the flow over a backward-facing step investigated experimentally by Pronchick and Kline [1]. The results predicted using the present approach are in good agreement with data.

## I. INTRODUCTION

The flow in most practical combustion devices, such as in gas turbine combustors, is characterized by recirculation zones, swirl, and strong interaction between turbulence and reaction. Predictions of turbulent flows, reacting and nonreacting, require the use of turbulence models to overcome the turbulence closure problem [2]. For reacting flows, additional closures are needed due to the nonlinear reaction rates and large density variations. The turbulence/chemistry interaction--the effect of turbulence on mean reaction rates and the effect of heat release due to reaction on the turbulence--is one of the least understood aspects of turbulent reacting flows [3].

The turbulence closures used currently are the mean-flow closure (e.g., k-ε model [4], Reynolds stress--algebraic (RSA) [5, 6, 7] models) and the second-order closures (e.g., Reynolds stress--differential (RSD) [8, 9]). In mean-flow closures, the Reynolds stresses (which transport momentum) are modeled, and in second-order closures, the triple velocity correlations (which transport Reynolds stresses) are modeled. These transport processes are usually modeled by gradient diffusion. The same ideas are used in modeling scalar transport as well. The conventional models can treat reactions only under special circumstances--when the reaction rate is linear or when it is very fast (e.g., [10]) or very slow compared with the turbulent time scale [11]. Also, sometimes these models involve an assumed form for the PDF of an appropriate scalar variable (e.g., [10]). However, a general nonlinear finite-rate reaction eludes treatment by these conventional models.

Since the first extensive application of analytical models as a design aid [12], based primarily on the k-ε model, a number of model improvements and combustor analytical design procedures have been proposed, but none of these has shown a consistently significant improvement over the basic approach [13]. Although the utility of the current models should not be overlooked, there is clearly a need to develop radically new and alternative methods for calculating turbulent recirculating and reacting flows. A most promising alternative is the PDF transport approach [14].

The joint probability density function (JPDF or PDF for short) transport approach [14] involves the solution of the evolution equation of the velocity-composition joint PDF. The joint PDF, $f(\underline{V}, \underline{\psi}; \underline{x}, t)$, is the probability density of the simultaneous event $\underline{U}(\underline{x}, t) = \underline{V}$ and $\underline{\phi}(\underline{x}, t) = \underline{\psi}$, where $\underline{U}$ is the velocity vector, $\underline{\phi}$ is a set of scalars, and $\underline{V}$ and $\underline{\psi}$ are independent variables in the velocity-scalar space.

The PDF transport approach overcomes most of the serious closure problems previously mentioned. The terms involving convection, reaction, body forces, and the mean pressure gradient (including the variable-density effects in those terms) appear in closed form. Hence, the use of conventional turbulence models (and consequently the gradient transport assumptions) is avoided. Also, arbitrarily complex reactions can be treated without approximations. It should be noted that the PDF transport method is different from the assumed PDF method in that the form of the PDF of the scalar is not assumed. Rather, the joint PDF of velocities and scalars is obtained from the solution of the transport equation for the PDF. An additional advantage of the PDF transport

approach is that the joint PDF contains a rather complete representation of the flow field, and any single-point correlation can be determined. This contrasts with conventional methods in which only a limited number of moments (usually the first and the second) of the PDF are determined.

The PDF f is a function of a large number of variables, 7 + $\sigma$--three velocity components, three space variables, time, and $\sigma$ scalars. Due to the large dimensionality of the PDF, standard techniques (such as finite differences to solve the PDF transport equation) are prohibitive [15]. Monte Carlo methods are computationally efficient in solving the transport equation and have been used for calculating many flows, some of which are listed in the next paragraph.

Some of the flows studied using the PDF transport method include plane jets [16], thermal wakes [17], evolution of homogeneous turbulence [18], mixing layers between turbulent streams of different length scales [19], self-similar turbulent free shear flows [20], premixed turbulent flames [21, 22, 23], and syngas diffusion flames [24]. These studies have clearly demonstrated the advantages offered by this method over conventional methods. However, the flows studied can be classified as simple flows--primarily time-dependent one-dimensional or two-dimensional boundary-layer type flows. It is necessary to apply the PDF transport method to more complex flows, such as confined, recirculating, swirling, and reacting flows, for it to be useful as a design tool for practical combustors.

The PDF transport method is described briefly in Section II. Although there are no theoretical restrictions for applying the method to multidimensional flows, there are certain limitations for making routine calculations of multidimensional flows, due to computer resource requirements. A novel approach, which combines the simplicity of conventional finite-volume solution algorithms for mean-flow equations and the advantages of the solution of the PDF transport equation, is presented in Section III. The approach is used to calculate the flow over a backward-facing step. The setup, results, and discussion are presented in Section IV. Section V presents the conclusions and directions for future work.

## II. THE PDF TRANSPORT METHOD

The reader is referred to the review paper by Pope [14] for the details of the derivation and the solution of the PDF transport equation, and to the work of Anand [25] for additional details on computations for turbulent reacting flows. A brief review is presented in the following paragraphs.

The evolution of the reactive flow field is governed by the conservation equations of mass (continuity), momentum, chemical species, and enthalpy. They are:

$$\frac{\partial \rho}{\partial t} + \frac{\partial}{\partial x_i}(\rho U_i) = 0, \tag{1}$$

$$\rho \frac{DU_j}{Dt} = \frac{\partial \tau_{ij}}{\partial x_i} - \frac{\partial p}{\partial x_j} + \rho g_j, \tag{2}$$

and

$$\rho \frac{D\phi_\alpha}{Dt} = - \frac{\partial J_i^\alpha}{\partial x_i} + \rho S_\alpha, \quad \alpha = 1,2,\ldots\sigma, \tag{3}$$

where the material derivative (the rate of change following the fluid) is

$$\frac{D}{Dt} = \frac{\partial}{\partial t} + U_i \frac{\partial}{\partial x_i} .$$

In these equations, $g_j$ is the body force (per unit mass) in the $x_j$-direction; $\tau_{ij}$ is the sum of the viscous and viscous-diffusive stress tensors, $S_\alpha$ is the source for the scalar $\phi_\alpha$ due to reaction, or in the case of the scalar being enthalpy, it is the source for specific enthalpy due to compressibility, viscous dissipation, and radiation; $\underline{J}^\alpha$ is the diffusive mass flux vector of species $\alpha$ (or the specific energy flux vector due to molecular transport for the scalar being enthalpy). A set of $\sigma$-scalars is considered, where there is no specific limitation on $\sigma$. For a given reference pressure $p_o$ (assumed constant), the density and sources depend only on the set of scalars $\underline{\phi}$:

$$\rho = \rho(\underline{\phi}), \tag{4}$$

$$S_\alpha = S_\alpha(\underline{\phi}). \tag{5}$$

The set of $\sigma$ scalars, $\underline{\Phi}$, provides a complete description of the thermochemical properties of the reactive mixture. Many combustion problems involve a large number of species and consequently $\sigma$ is large. However, in idealized premixed and diffusion flames, the gas composition (by assumption) is determined by a single scalar. For constant-density, nonreacting flows, like the one considered in the present study, $\rho$ is a constant and $S_\alpha$ is zero.

The transport equation for the joint PDF can be derived from the set of conservation equations (1-3) and the definition of "expectation" or mean (see [14] for details). The resulting PDF transport equation is:

$$\rho(\Psi)\frac{\partial f}{\partial t} + \rho(\Psi)\,V_j\frac{\partial f}{\partial x_j} + \left(\rho(\Psi)g_j - \frac{\partial \langle p\rangle}{\partial x_j}\right)\frac{\partial f}{\partial V_j} + \frac{\partial}{\partial \psi_\alpha}\left[\rho(\Psi)S_\alpha(\Psi)f\right]$$

$$= \frac{\partial}{\partial V_j}\left[\left\langle -\frac{\partial \tau_{ij}}{\partial x_i} + \frac{\partial p'}{\partial x_j}\,\middle|\,\underline{V},\,\Psi\right\rangle f\right] + \frac{\partial}{\partial \psi_\alpha}\left[\left\langle \frac{\partial J_i^\alpha}{\partial x_i}\,\middle|\,\underline{V},\,\Psi\right\rangle f\right]. \quad (6)$$

The terms on the right side involve conditional expectations. The conditional expectation $\langle Q\,|\,\underline{V},\,\Psi,\,\underline{x},\,t\rangle$ is the expectation of the quantity Q at position $\underline{x}$ and time t on the condition that the velocity and the scalar values are $\underline{U}\,(\underline{x},\,t) = \underline{V}$ and $\underline{\Phi}\,(\underline{x},\,t) = \Psi$. If the conditional expectations appearing on the right side were known, the transport equation (6) could be solved for f ($\rho$ and $\underline{S}$ are known functions of $\Psi$ and the mean pressure $\langle p\rangle$ can be determined from f). However, the terms on the left-hand side of equation (6) are entirely "known" in terms of f and the independent variables $\underline{x}$, t, $\underline{V}$, and $\Psi$. Thus, all the processes represented by those terms are accounted for exactly, without any approximation. Those processes are: variation with time; transport in physical space (convection); effects of body forces, mean pressure gradient, and reaction, respectively. It is remarkable that in a variable-density flow with arbitrarily complicated reactions, all these processes can be treated without approximation. The terms on the right side of equation (6) represent transport in velocity space by the viscous stresses and by the fluctuating pressure gradient; and transport in composition space by the molecular fluxes, respectively. Before the equation can be solved for f, the conditional expectations appearing in those terms must be modeled.

The conditional expectation due to viscous stresses and fluctuating pressure gradients is modeled by the simplified Langevin model [17, 20]. The conditional expectation due to the molecular fluxes of scalars is modeled by the improved mixing model [26].

These models are usually prescribed as functions of the joint PDF and a specified turbulent time scale $\tau(\underline{x}, t)$. The modeled PDF transport equation is solved by a Monte Carlo method. As mentioned in Section I, this method has been successfully applied to many simple flows.

Theoretically, there is no restriction for extending the method to two-dimensional and three-dimensional flows; however, there are practical limitations. First, although the Monte Carlo method is vastly more efficient than finite-difference techniques for solving the PDF equations, it is still computer intensive for practical multidimensional flows. To reduce the statistical errors, a large number of stochastic (or computational) particles are needed in the Monte Carlo solution. Second, the mean pressure gradient (which appears in the transport equation for the PDF [equation 6]) can be calculated from the particle properties as a part of the solution by solving an elliptic equation for the mean pressure [14]. However, the accuracy to which some of the terms in the elliptic equation need to be determined further emphasizes the need for a large number of stochastic particles, especially for variable-density flows. The solutions may require several hundred thousand particles. The computational time increases nearly linearly with the number of particles, although the calculation of simple flows noted in Section I have typically required only a few minutes of CPU time on an IBM mainframe such as a 3081, but using only tens of thousands of particles. In view of these facts, a straightforward extension of the method described in this section will require computer resources which are not readily available to all but a few for making routine calculations of multidimensional flows. Further improvements in the method and the solution algorithm are expected to make such an extension of the PDF method much more affordable. In the present study, however, a simpler approach is presented as a first step to demonstrate the feasibility of the PDF method for multidimensional flows.

## III. PRESENT APPROACH

An approach which exploits both the simplicity of the SIMPLE-based finite-volume (FV) algorithm [27] for the solution of the Reynolds-averaged flow equations and the modeling advantages of the PDF transport approach is presented in this section as a viable tool for analyzing complex multidimensional flows.

The basic idea behind the approach is to take advantage of the PDF method's capability for calculating higher order correlations (such as Reynolds stresses) rather than expend considerable computational effort in computing the mean pressure field. The mean pressure field is more easily calculated using the SIMPLE-based finite-volume algorithm. This results in a very significant reduction in the computer resources needed and makes the method feasible. However, the basic idea has to be carefully incorporated to achieve consistent results.

The ultimate objective of this approach is to develop a Monte Carlo code to solve a modeled joint PDF equation for multidimensional elliptic turbulent reacting flows. The immediate objective is to couple the Monte Carlo method with the finite-volume (FV) algorithm to solve for the joint PDF. The theme of the approach is to start with the FV code and to superimpose the Monte Carlo method.

The Monte Carlo and the finite-volume codes are linked in the following manner. The FV code supplies the Monte Carlo code with the mean velocity, the turbulent time scale ($\tau$), and the mean pressure fields. The turbulent time scale, $\tau$ ($= k/\varepsilon$, where k is the turbulent kinetic energy and $\varepsilon$ is its rate of dissipation), is needed for the Langevin and the stochastic mixing models mentioned in Section II. The need to transfer the mean pressure field has already been discussed. Given the mean pressure field and the turbulent time scale, the Monte Carlo code can compute the mean velocities and all the other statistics. However, the mean velocity field is still transferred and the mean velocity field computed by the Monte Carlo code is periodically adjusted to correspond to that provided by the FV code. This is done to keep the mean velocity consistent with the mean pressure field.

The Monte Carlo code in turn supplies the Reynolds stresses and k (computed by the Monte Carlo code) to the FV code. The Reynolds stresses are incorporated in the momentum equations in the FV code, thus eliminating the need for modeling the stresses through the k-$\varepsilon$ or the Reynolds stress models. The kinetic energy field supplied by the Monte Carlo code is held fixed in the FV code while $\varepsilon$ is computed.

The sequence of solution is as follows. A converged solution of the flow field is obtained with the FV code using one of the conventional models such as k-$\varepsilon$ or Reynolds stress--algebraic (RSA) models. The required mean fields are transferred to the Monte Carlo code as initial conditions. After a steady-state solution is obtained with the Monte Carlo code, the necessary

quantities are transferred back to the FV code. Now the velocity and pressure fields are perturbed due to the new stresses. The entire process is repeated until the fields are no longer perturbed beyond a specified limit upon return from the Monte Carlo code.

For the case of variable density flows (reacting and non-reacting), the mean density field is also shared by the two codes.

Before the approach just described can be used to compute confined flows, the treatment of solid boundaries (walls) in the Monte Carlo code has to be addressed. The flows studied previously using the Monte Carlo method did not have solid boundaries to be treated in the solution domain. Pope [28] recently developed the treatment for walls and applied it successfully for calculating the developing turbulent flow through a pipe. The essence of the treatment is presented here while the details are omitted. The treatment ensures that the stochastic particles in the Monte Carlo solution lose the required amount of momentum at the wall so that the resulting shear stress and mean velocity profiles near the wall are consistent with the log-law of the wall. The wall treatment has been incorporated in the present study for calculating confined recirculating flows.

## IV. RESULTS AND DISCUSSION

The approach described in Section III was applied to the planar flow over a backward-facing step investigated experimentally by Pronchick and Kline [1]. The schematic of flow is shown in Figure 1. The flow enters through the inlet channel of height $(W_1 + W_2)$ and flows over a step of height H into an expanded channel of height $W_3$ $(= W_1 + W_2 + H)$. A recirculation zone results just behind the step, and the distance of the reattachment point from the step, defined as the reattachment length, is denoted by $x_R$. The problem shown in Figure 1 is a slight variant of the problem studied by Pronchick and Kline. In their case, the inlet is a single passage of height $(W_1 + W_2)$ and a single fluid (water) flows through the inlet at a Reynolds number of 12,000 based on the step height H and the centerline velocity in the inlet channel $(U_{ref})$. In the present study, a scalar (say fuel) is introduced through part of the inlet channel over the height $W_2$ as shown in Figure 1. The fuel is chosen, for simplicity, to be of nearly the same density as the fluid through the other part of the inlet channel (the primary fluid). For

example, with air as the primary fluid, the choice of fuel is CO. The Reynolds number is maintained at 12,000 so that the fluid dynamics of the two problems is identical. The width over which the fuel, say CO, is introduced was determined such that the overall equivalence ratio is equal to 1.0. Thus, defining the mass fraction of CO to be the scalar $\phi$, the value of $\phi$ is unity in the upper stream and zero in the lower stream at the inlet.

The computational domain extended from the step (inlet) to 15 step-heights downstream of the step, bounded by the top and bottom walls. Fully developed profiles for mean velocity, kinetic energy, and dissipation were used at the inlet. The profiles were based on the full inlet channel height ($W_1 + W_2$), assuming the wall separating the scalar stream to be a full-slip wall, to be consistent with Pronchick and Kline's experiments.

The results are presented in Figures 2 through 11. The transverse profiles of various quantities are plotted at different streamwise locations. The normalized streamwise coordinate $x^*$ is defined by

$$x^* = \frac{(x - x_R)}{x_R} \tag{7}$$

where x is the distance from the step (Figure 1) and $x_R$ is the reattachment length. This choice of normalized streamwise coordinate for comparing profiles is suggested, among others, by Westphal et al. [29] and Pronchick and Kline [1].

The streamwise stations shown in the figures consist of two stations in the recirculation region, the third near the reattachment point, and the fourth in the redevelopment region downstream of the reattachment point. The PDF results are also contrasted with the results from the k-ε model in Figures 1 through 3. The reattachment length obtained are (as multiples of the step-height):

- o k-ε--4.8H
- o PDF--5.3H
- o experiment--6.75H

Traditional finite-volume calculations generally tend to predict a lower value for the reattachment length than that observed experimentally. It has been shown that a part of the reason for this is the numerical diffusion introduced by the hybrid differencing scheme used here in the finite-volume calculations. The use of higher order differencing schemes results in improved

predictions for the reattachment length [30, 31]. The second reason for the lower reattachment length is the turbulence model used. In this respect, it is encouraging to note that the PDF calculation shows considerable improvement over the k-ε model. However, this result could be fortuitous, and further investigation is necessary.

Figures 2 and 3, respectively, show the mean streamwise velocity (<U>) and mean transverse velocity (<V>) profiles normalized by $U_{ref}$. The streamwise velocity profiles are uniformly in good agreement with data. Also, the profiles calculated by the k-ε model and those by the present PDF approach are nearly the same although some differences are evident. The agreement of the calculated profiles for transverse mean velocity with data is moderate. The calculated profiles do display the qualitative features of the experimental data. It should be recognized that the transverse velocities are an order of magnitude lower than the streamwise velocities.

Figure 4 shows the kinetic energy (k) profile, and Figure 5 shows the streamwise velocity variance ($\langle u'^2 \rangle$) profiles. The profiles are normalized by $U^2_{ref}$. No experimental data are available for the kinetic energy. However, the kinetic energy is of the same order as $\langle u'^2 \rangle$ in these flows. The k-ε model predicts higher values of the kinetic energy than the PDF calculations. Given the agreement between the PDF calculations and data for $\langle u'^2 \rangle$ seen in Figure 5, and for $\langle v'^2 \rangle$ seen in Figure 6, it is reasonable to assume that the kinetic energy calculated from the PDF is closer to the actual experiment and that the k-ε model overpredicts the kinetic energy.

Figure 5 shows that the calculated PDF accurately predicts the locations of the peaks in the streamwise velocity variance profiles at all stations though the magnitudes of the peaks do not match the data exactly. The same observation is true for the transverse velocity variance profiles shown in Figure 6. Nevertheless, the calculated variances are generally in good agreement with data.

The turbulent shear stress ($\langle u'v' \rangle$) profiles calculated from the PDF are compared against data in Figure 7. The profiles are normalized by $U^2_{ref}$. Again, the peak locations are well predicted while there are some differences in magnitude between predictions and data. The agreement is still quite satisfactory. Further, the agreement of the computed and measured shear stresses near the wall lends support to the wall treatment used in the Monte Carlo calculations.

Figures 8 through 11 show various third-order velocity correlations normalized by $U_{ref}^3$. The values calculated from the joint PDF compare well with data. The agreement further implies that the shapes of the PDFs from calculations and experiments are in good agreement at least up to the third moments. The agreement between the calculated profiles and the data for the third order correlations is especially noteworthy since the third-order correlations are one to two orders of magnitude smaller than the second-order correlations, and three to four orders of magnitude smaller than the mean velocities.

We now present the results of the scalar calculations. Though data is not available for comparison, the calculations are presented to demonstrate the capability for scalar calculations using the present approach. In fact, the scalar calculations with the present approach are no different from the fully Monte Carlo based calculations used for the flows referred to in Section II. For the present problem, the scalar calculations were performed entirely in the Monte Carlo part of the code.

Figures 12 through 15 present the calculated profiles for the mean, variance, streamwise flux, and transverse flux of the scalar (fuel mass-fraction), respectively. The figures show the expected trends. The peaks of the mean and variance (Figures 12 and 13) occur at the expected locations, consistent with the inlet conditions and the computed velocity field. The scalar fluxes in Figures 14 and 15 are consistent with the mean scalar and velocity fields.

Some information on the computational times is given in this paragraph only to give the reader an idea of the CPU times involved and to demonstrate that the method is indeed affordable. A set of finite-volume calculations followed by the Monte Carlo calculations is termed a cycle. The Monte Carlo code takes approximately 45 seconds of CPU time for 50 time-steps with 100,000 particles on a CRAY-XMP, which is typical of the runs made for each cycle. This time reflects a moderate effort to vectorize the code as well as improve the Monte Carlo algorithm, resulting in substantial reductions in the CPU time required since the initial formulation of the approach. The finite-volume calculations were performed on an IBM 3084. Typically, about 200 iterations are performed with the FV code for each cycle, requiring approximately 2 minutes of CPU time. Taking into account the difference in execution speeds between the CRAY and the IBM, it is seen that the computational times for the Monte Carlo and the finite-volume codes are of the same order of magnitude. Usually two or three cycles of calculations are sufficient for obtaining a converged

solution, i.e., one that is not perturbed significantly upon return from the Monte Carlo calculations. A systematic study of the optimum number of particles required or the optimum number of time-steps or iterations required during each cycle has not been performed.

## V. CONCLUSIONS

A PDF method for calculating turbulent recirculating flows has been proposed, and for the first time joint PDF calculations for such flows have been performed. The results of the calculations for the flow over a backward-facing step show good agreement with experimental data of Pronchick and Kline [1]. The proposed method is applicable to turbulent recirculating and reacting flows such as in gas turbine combustors and other practical combustion devices.

Several developmental tasks for the method can be identified. The developments can be classified into two areas--improvements to existing models or development of new models, and improvements to the solution algorithm. One of the objectives of the present approach is to progressively eliminate the dependence on the finite-volume code and solve the joint PDF equation entirely by the Monte Carlo method. Two important aspects (rather, limitations) of the method have to be addressed to achieve this goal. They are the need to supply a turbulent time scale externally and the determination of the mean pressure gradient.

There has been some preliminary work on determining the rate of viscous dissipation ($\varepsilon$) within the Monte Carlo solution [19]. This is done by treating $\varepsilon$ as one of the scalar variables of the PDF so that the mean dissipation rate can be determined from the PDF (i.e., from the properties of the stochastic particles in the solution). This particle-dependent dissipation model needs to be further developed and tested. With the advances in the capability of the current computers in regard to available storage and speed, and with further improvements to the Monte Carlo algorithm for determining the mean pressure field, it will be possible to eliminate the need to supply the mean pressure field from the finite-volume code. Some progress has already been made in this respect. Preliminary results, obtained by the present authors, from improvements to the solution algorithm have shown that the mean pressure field can be computed within the Monte Carlo solution with moderate computational effort.

27. S. V. Patankar, Numerical Heat Transfer and Fluid Flow, Hemisphere, 1980.
28. S. B. Pope, Private communication, Cornell University, Ithaca, New York, 1987.
29. R. V. Westphal, J. P. Johnston, and J. K. Eaton, "Experimental Study of Flow Reattachment in a Single-Sided Sudden Expansion," NASA CR-3765, January 1984.
30. S. V. Patankar, K. C. Karki, and H. C. Mongia, "Development and Evaluation of Improved Numerical Schemes for Recirculating Flows," AIAA 87-0061.
31. S. Syed and L. Chiappetta, "Finite Difference Methods for Reducing Numerical Diffusion in TEACH-Type Calculations," AIAA 85-0057.

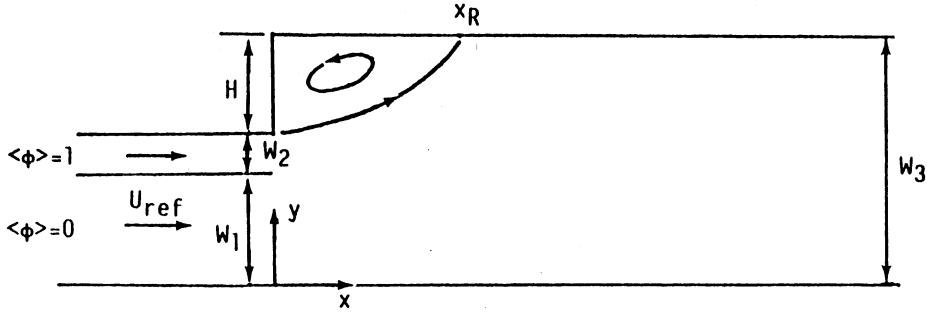


H = 0.0762 m
$W_1$ = 0.1186 m
$W_2$ = 0.0592 m
$W_3$ = 0.254 m

$W_3/(W_2+W_1)$ = 1.43

$U_{ref}$ = 0.196 m/s

Figure 1: Schematic of the backward-facing step with a fuel stream.

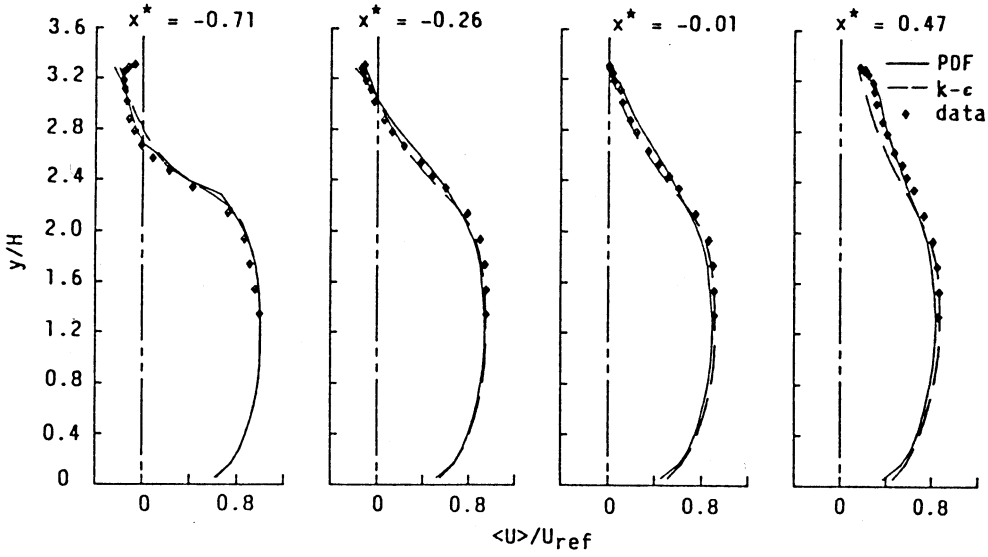


Figure 2: Predicted mean streamwise velocity profiles compared against data [1].

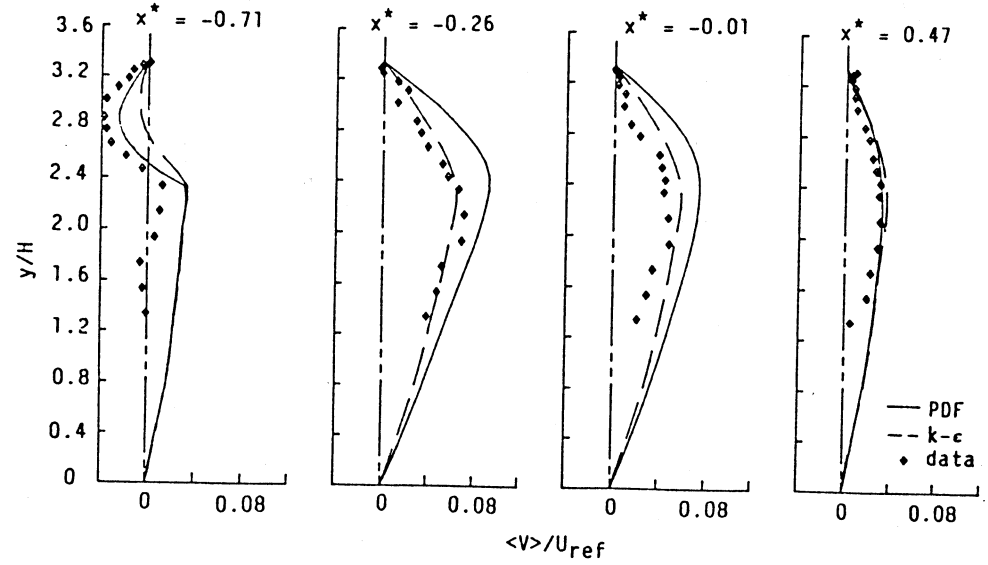


Figure 3: Predicted mean transverse velocity profiles compared against data [1].

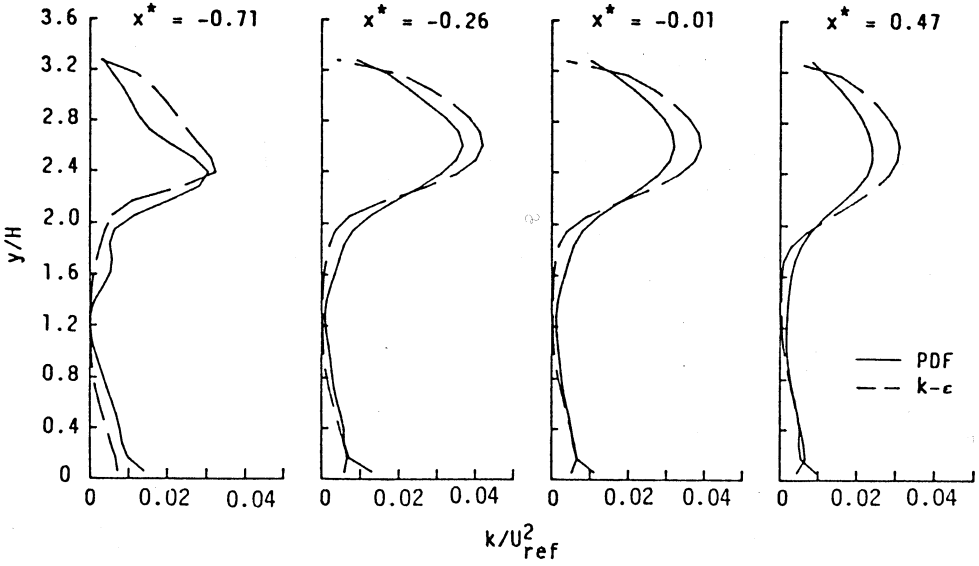


Figure 4: Predicted kinetic energy profiles.

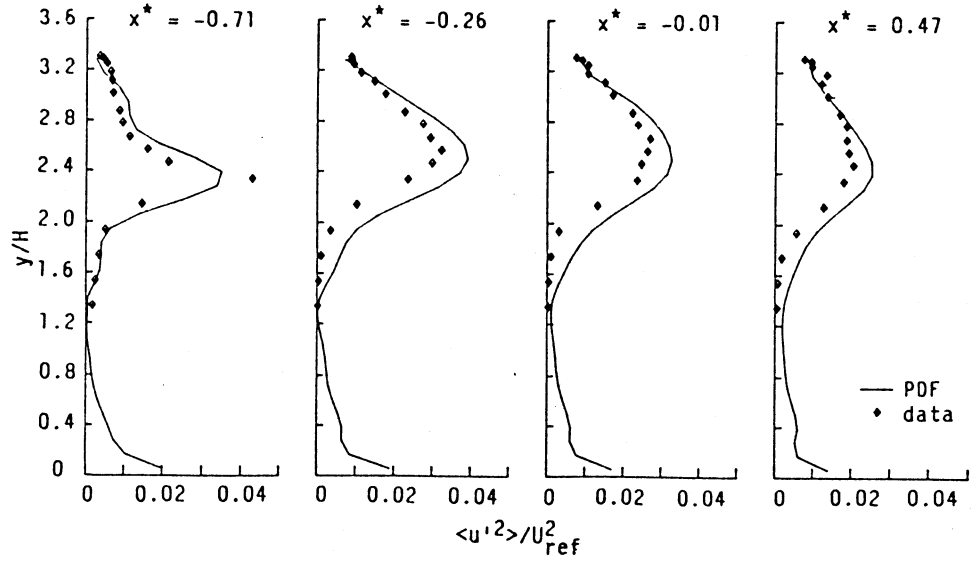


Figure 5: Predicted streamwise velocity variance profiles compared against data [1].

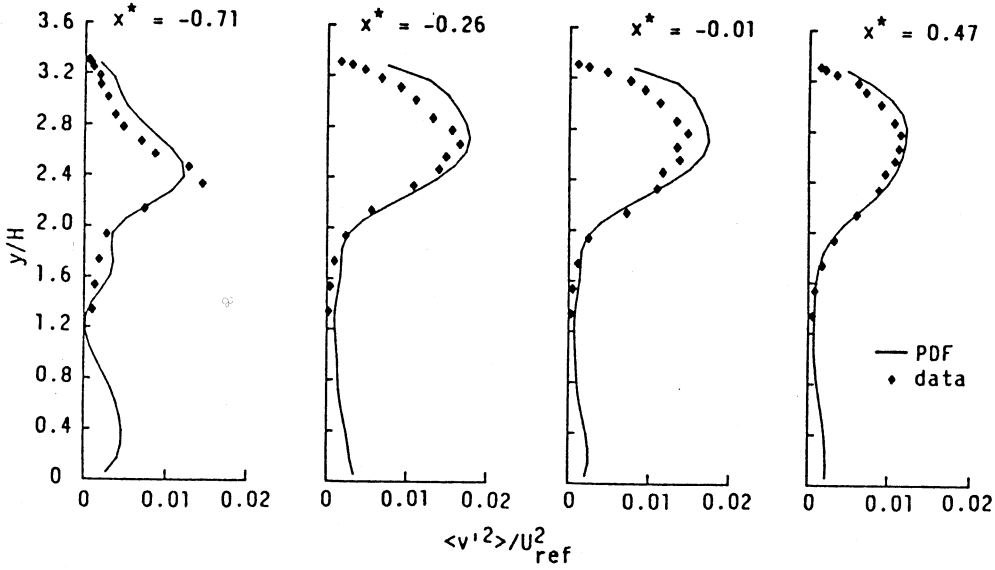


Figure 6: Predicted transverse velocity variance profiles compared against data [1].

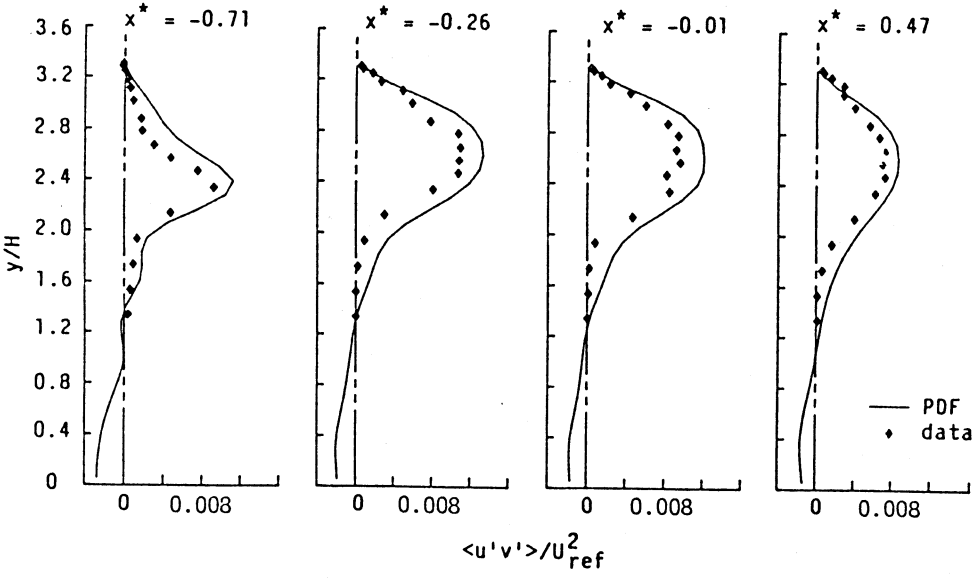


Figure 7: Predicted shear stress profiles compared against data [1].

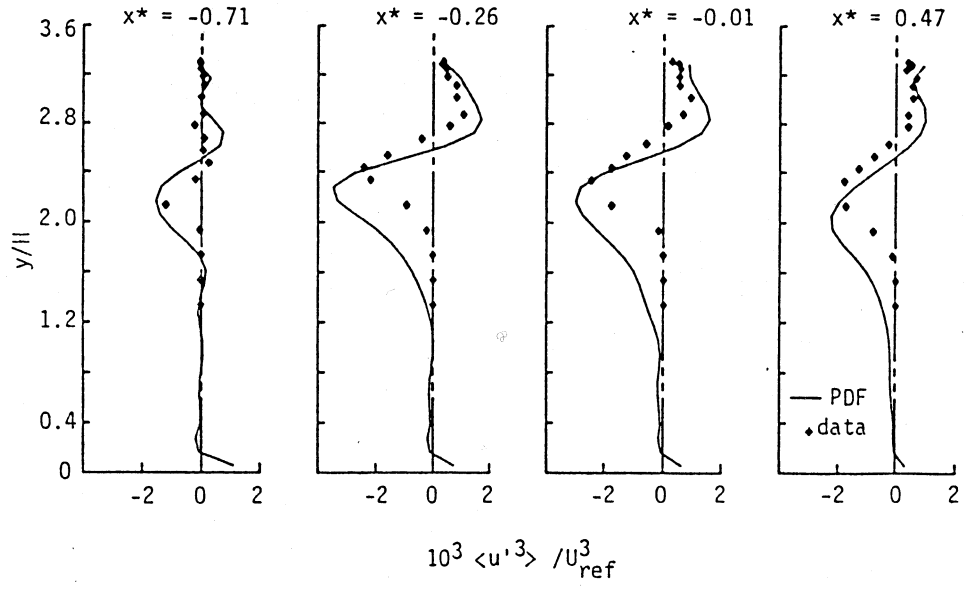


**Figure 8: Predicted $\langle u'^3 \rangle$ profiles compared against data [1].**

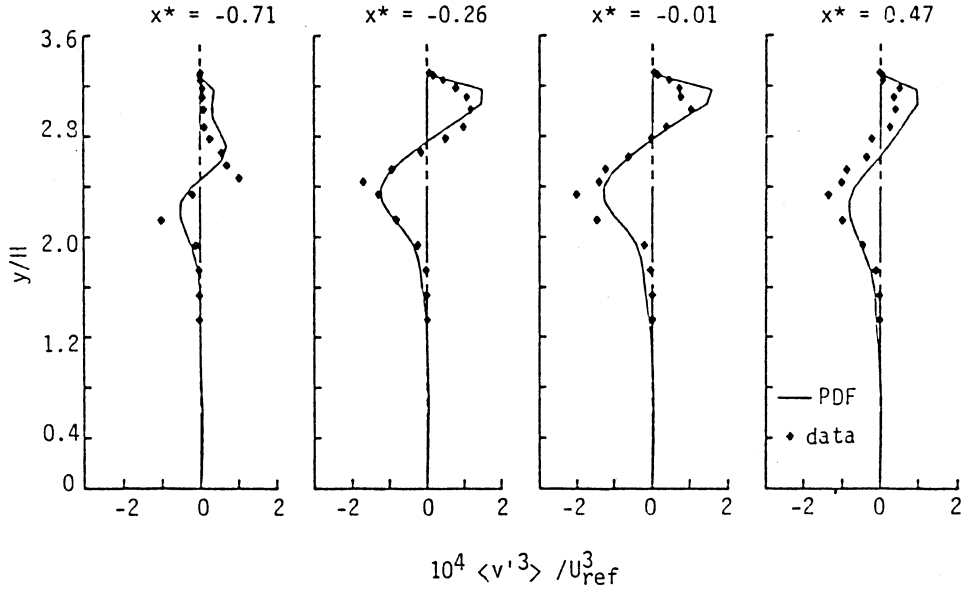


**Figure 9: Predicted $\langle v'^3 \rangle$ profiles compared against data [1].**

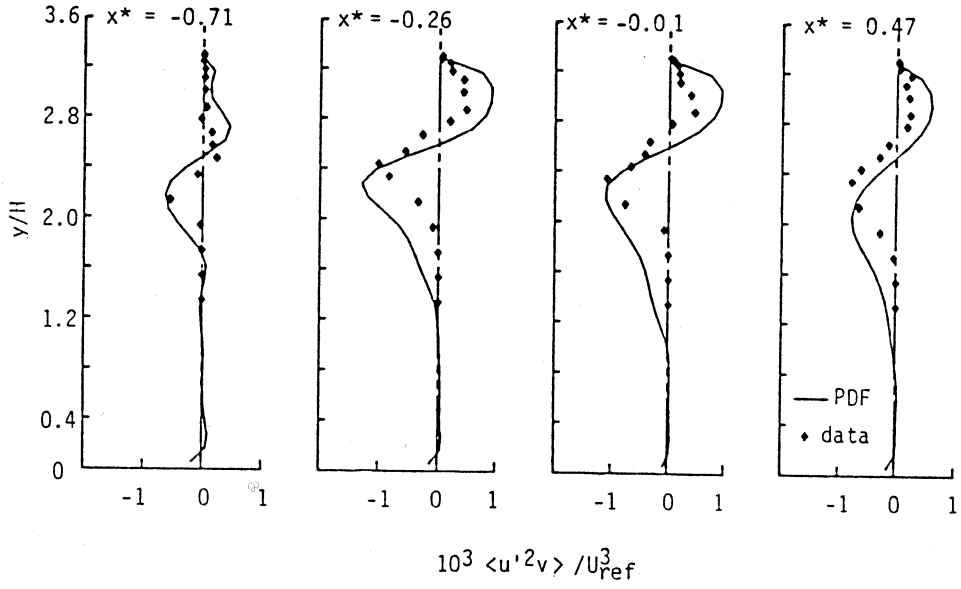


Figure 10: Predicted $\langle u'^2 v' \rangle$ profiles compared against data [1].

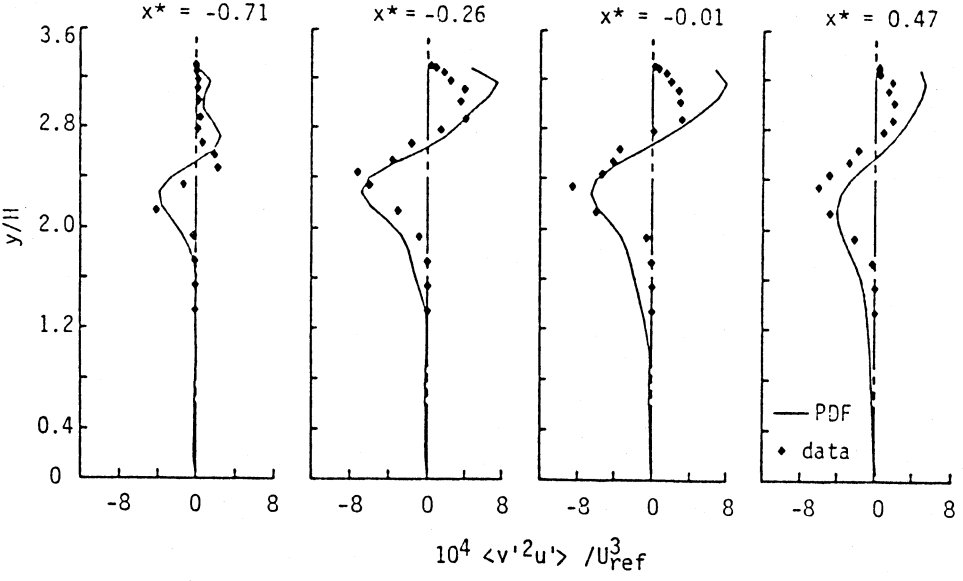


Figure 11: Predicted $\langle v'^2 u' \rangle$ profiles compared against data [1].

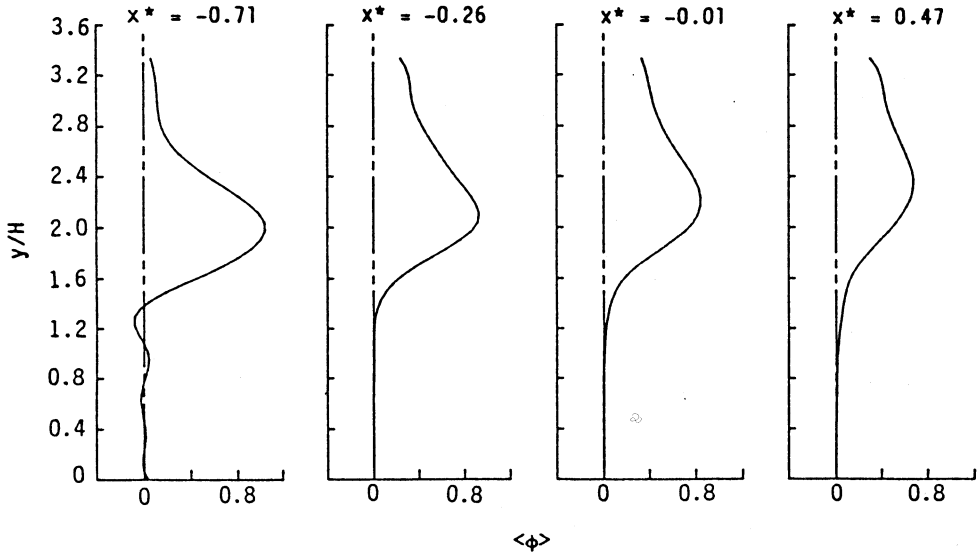


Figure 12: Predicted profiles of mean fuel mass-fraction.

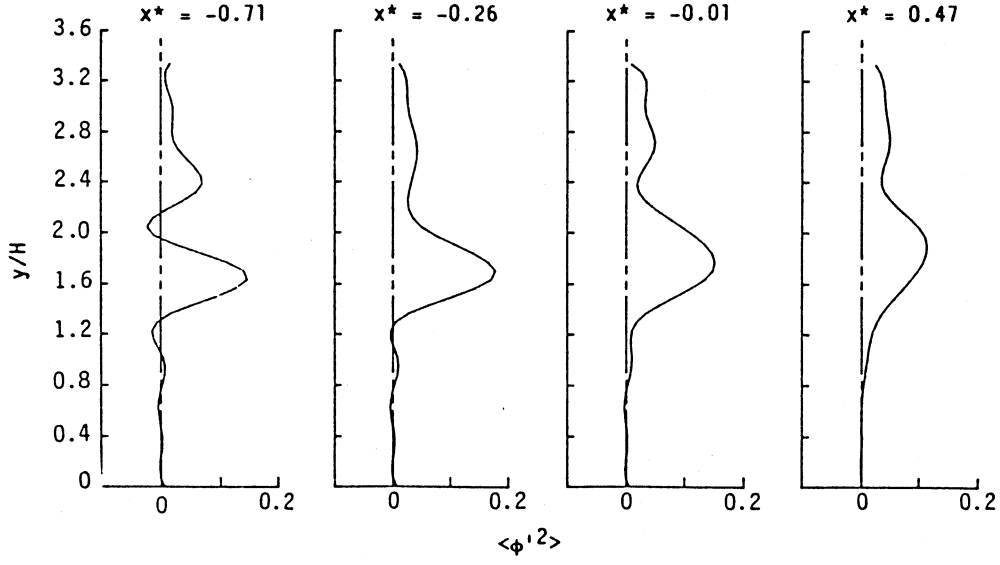


Figure 13: Predicted profiles of the variance of fuel mass-fraction.

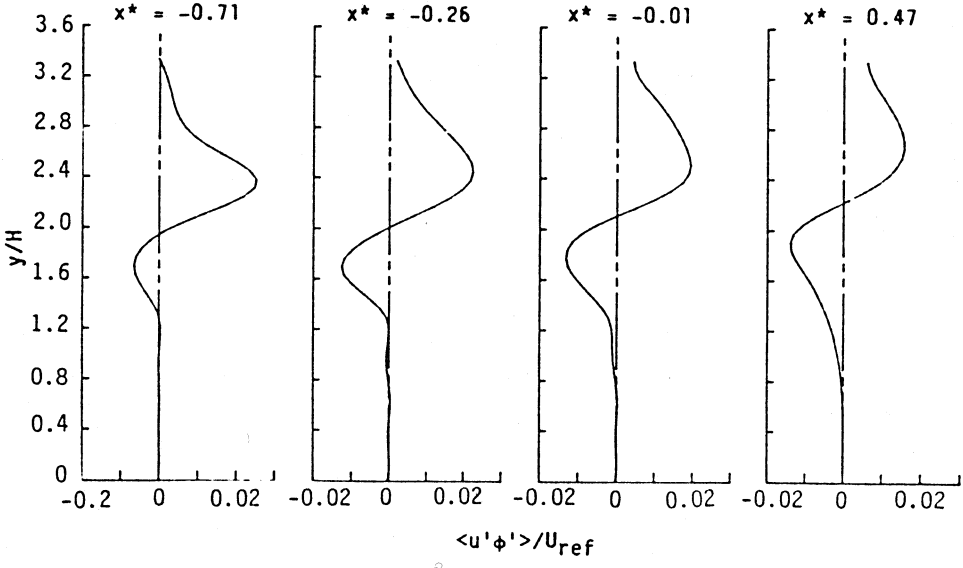


Figure 14: Predicted profiles of streamwise flux of fuel mass-fraction.

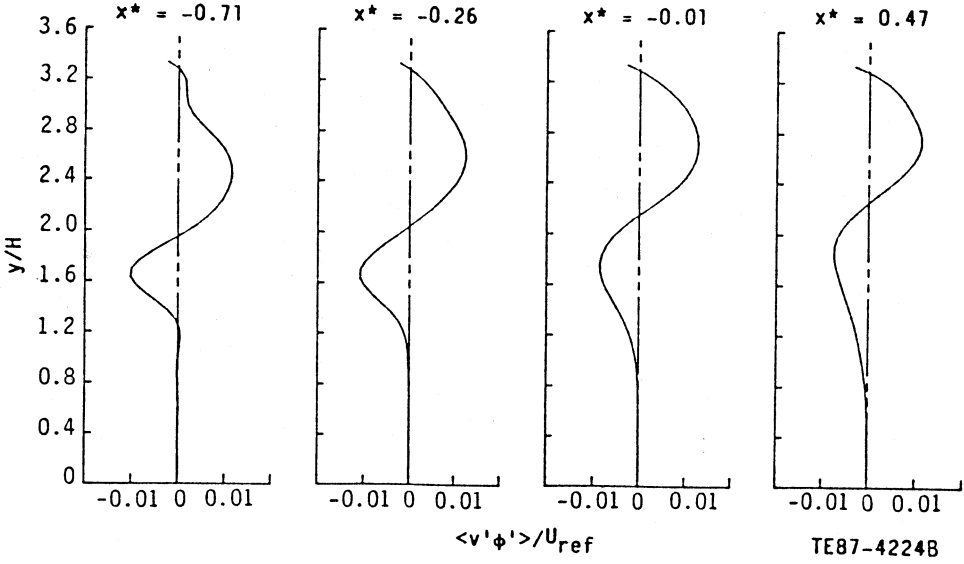


Figure 15: Predicted profiles of transverse flux of fuel mass-fraction.